

# Accurate Evaluation of RCS on the Structure of Aircraft Inlets

Jingyan Mo<sup>1,2</sup>, Weidong Fang<sup>2</sup>, Haigao Xue<sup>2</sup>

1 Shanghai Aerospace System Engineering Institute

2 School of Communication and Information Engineering, Shanghai University  
Shanghai, 200021, China, mojingyan@163.com

Ying Yan

School of Electronic Engineering, Xidian University  
Xi'an, 710071, Shaanxi, China, yymqn1008@163.com

Zhewang Ma

Graduate School of Science and Engineering, Saitama University  
255 Shimo-Okubo, Sakura-ku, Saitama-shi, Saitama 338-8570, Japan

**Abstract-** A parallel version of Method of Moments (MoM) with Higher-Order Basis functions (HOB-MoM) with the Out-of-Core technique (OOC) is proposed to compute the Radar Cross Section (RCS) of an aircraft with engine inlets in this paper. The block-partitioned parallel scheme for the large dense MoM matrix is designed to achieve excellent load balancing and high parallel efficiency. The OOC technology is employed to break through the random access memory (RAM) limitation. Some numerical results demonstrate that the higher-order basis used in this paper is superior to the conventional RWG basis and is suitable to solve various electrically large problems such as the computation of RCS.

## I. INTRODUCTION

Radar Cross Section (RCS) computation of complex large structures has been paid more and more attention in vehicle stealth design. Recently, so many numerical methods, such as Finite Element Method (FEM), Finite Difference Time Domain (FDTD), Finite Integral Time Domain Method (FITD), Fast Multi-pole Method (FMM), MoM [1] are used to compute RCS. However, as the simulation frequency becomes higher, the MoM method based on Rao-Wilton-Glisson basis functions (RWGs) [3, 5] produces a large number of matrix unknowns for electrically large complex structures. To reduce the number of unknowns and to accelerate the computation, the fast multi-pole method (FMM) is a feasible approach. But when the complex cavity structure such as aircraft's engine is considered, the convergence of FMM may be a problem. For such structures, both the techniques of FEM and FDTD [7] have the huge working amount to finish the discretization, which will also produce large number of unknowns. To handle this problem, another choice is to use MoM with Higher-Order basis (HOB-MoM), which can significantly reduce the number of unknowns. But unfortunately, HOB-MoM still requires much memory for the simulation of large complex structures. Thus, OOC technology is of great value.

In stealth aircraft design, the engine inlet is a main scattering source to be considered. Typical engine inlet is a one-end open waveguide cavity with large size for radar frequency and radar waves entering in it will have severe

effect of resonance and multi-reflect. For this kind of structures, the FMM will spend more simulation time and iteration steps to obtain a stable and accurate solution. HOB-MoM is a good choice to deal with this type of problems.

Apart from the section of introduction, the second section of this paper presents the basic theory used in this paper; Section three presents some numerical examples to validate the capacity and application of this paper's method; Finally, Section four gives the conclusion.

## II. BASIC THEORY

### 1. Higher Order Basis Functions

Flexible geometric modelling can be achieved by using truncated cones for wires and bilinear patches to characterize surfaces [2]. The surface current over a bilinear surface is decomposed into its p and s-components, as shown in Fig.1 (a). The p-current component can be treated as the s-current component defined over the same bilinear surface with an interchange of the p and s coordinates. The approximations for the s-components of the electric and magnetic currents over a bilinear surface are typically defined by:

$$\vec{J}_s(p, s) = \sum_{i=0}^{N_p} [c_{i1} \vec{E}_i(p, s) + c_{i2} \vec{E}_i(p, -s)] + \sum_{j=2}^{N_s} a_{ij} \vec{P}_{ij}(p, s) \quad (1)$$

Where  $c_{i1}, c_{i2}, (i = 0, 1, \dots, N_p)$  are defined as

$$c_{i1} = \sum_{j=0}^{N_s} a_{ij} (-1)^j, c_{i2} = \sum_{j=0}^{N_s} a_{ij} \quad (2)$$

The edge basis functions  $\vec{E}_i(p, s)$  and the patch basis functions  $\vec{P}_{ij}(p, s) (i = 0, \dots, N_p, j = 2, \dots, N_s)$  are expressed by (3) and (4) respectively

$$\vec{E}_i(p, s) = \frac{\vec{\alpha}_s}{|\vec{\alpha}_p \times \vec{\alpha}_s|} p^i \vec{N}(s) \quad (3)$$

$$\vec{P}_{ij}(p, s) = \frac{\vec{\alpha}_s}{|\vec{\alpha}_p \times \vec{\alpha}_s|} p^i \vec{S}_j(s) \quad (4)$$

where  $\vec{\alpha}_p, \vec{\alpha}_s$  are the unitary vectors defined as

$$\bar{\alpha}_p = \frac{\partial \bar{r}(p,s)}{\partial p}, \bar{\alpha}_s = \frac{\partial \bar{r}(p,s)}{\partial s} \quad (5)$$

The parametric equation of such an isoparametric element can be written in the following form as

$$\bar{r}(p,s) = \bar{r}_{11} \frac{(1-p)(1-s)}{4} + \bar{r}_{12} \frac{(1-p)(1+s)}{4} + \bar{r}_{21} \frac{(1+p)(1-s)}{4} + \bar{r}_{22} \frac{(1+p)(1+s)}{4} \quad (6)$$

$-1 \leq p \leq 1, -1 \leq s \leq 1$

where  $\bar{r}_{11}, \bar{r}_{12}, \bar{r}_{21}, \bar{r}_{22}$  are the position vectors of its vertices, and the  $p$  and  $s$  are the local coordinates.

A right-truncated cone is determined by the position vectors and the radii of its beginning and its end,  $\bar{r}_1, a_1, \bar{r}_2, a_2$ , respectively, as shown in Fig. 1 (b). Generalized wires (i.e., wires that have a curvilinear axis and a variable radius) can be approximated by right-truncated cones.

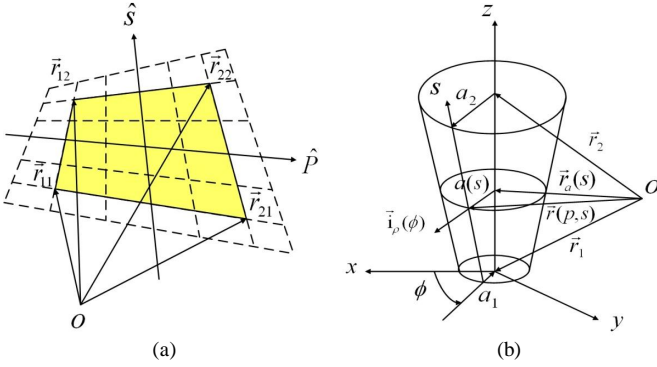


Figure 1. Geometric model: (a) A bilinear surface defined by four vertices

## 2. Out-of-Core factorization and solving

When the MoM matrix is too large to the computer at hand, the space of hard disk should be used to extend the storage capability. When the matrix is too large, they can be stored on the hard disk. As the matrix starts, one portion of the matrix is computed at a time and then written to the hard disk; another matrix portion will be computed and written, which will be repeated until the complete matrix filling has been finished. It is necessary to mention that, for the in-core matrix filling algorithm, the entire matrix is filled at one step, but need not be written out. The main idea of designing the out-of-core algorithm is to improve the performance of in-core algorithm. When performing the out-of-core LU factorization, each portion of the matrix is read into RAM and performs the LU decomposition respectively. Then the results after being factorized are written back to the hard disk. The code then precedes the next portion of the matrix until the whole matrix has been LU factored.

The decomposition in this paper is oriented along the column; each in-core filling is a slab of the matrix, as shown in Fig.2.

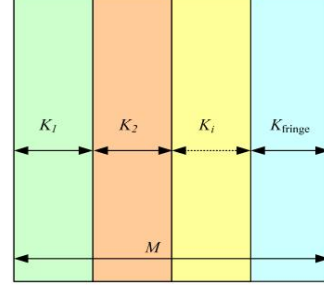


Figure 2. Data decomposition for storing an out-of-core matrix

The width of the  $i$ th out-of-core slab  $K_i$ , as illustrated in Figure 2, is bounded by

$$M = \sum_{i=1}^{I_{slab}} K_i \quad (7)$$

At the last out-of-core fill ( $i=I_{slab}$ ), the number of unfilled columns is

$$M_{fringe} = M - \sum_{i=1}^{I_{slab}-1} K_i \quad (8)$$

When only one process is used, the out-of-core matrix filling can easily be done with a slight modification to the serial code. However, when more processes are used, the assignment to fill each slab is distributed over  $p$  processes by using the block distribution scheme of ScaLAPACK [2]. Thus, the matrix filling schemes need to be designed in such a way so as to avoid redundant calculation for better parallel efficiency.

## III. NUMERICAL EXAMPLES

### 1. Comparison with the measurement results

To validate the accuracy and efficiency of the proposed parallel Higher-order basis MoM methodology, a benchmark of a truncated cone is simulated to compare its RCS results with those from the measurement.

The model simulated is an end-capped truncated cone oriented along the  $z$ -axis and centred in the plane  $z = 0$  (illustrated in Fig. 3). The elevation angle ( $\theta$ ) is taken from the positive  $z$ -axis and the azimuth angle ( $\phi$ ) from the positive  $x$ -axis. There are several interesting points about this target. First, it shows the RCS response of targets with single curvature (common in structural parts of an aircraft, such as the fuselage). It is also important to know the diffraction mechanism at curved edges. Reflection from planar surfaces with curved edges can also be observed. Therefore, this target is especially suitable for the validation of the prediction of objects with flat surfaces delimited by curved edges and for evaluation of curved edge contributions.

The model is simulated at 7 GHz. The RCS pattern for HH polarizations and corresponding to  $\phi = 0$  and  $\theta = 0^\circ \sim 180^\circ$  is simulated. The incident direction is perpendicular to the generatrix.

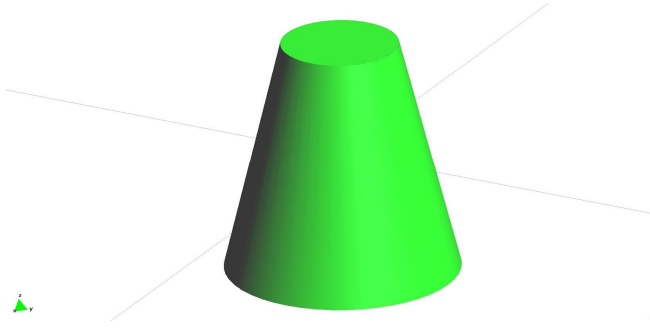


Figure 3. Truncated cone description: size (in mm). The height of the target is 200 mm. The major diameter is 200mm and the minor one is 100mm.

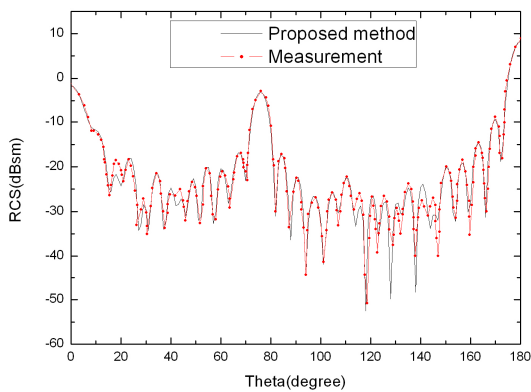


Figure 4. RCS pattern of the truncated cone. Frequency: 7GHz. Polarization: HH. Comparison with Measurement.

Fig. 4 shows the RCS results we wish to observe, from which we can find there are three main lobes. Two of them correspond to the specular reflection from the two bases of the cone. The minor one corresponds to  $\theta = 0^\circ$  and the major one to  $\theta = 180^\circ$ , they are of the different levels resulting from the different areas of the corresponding bases. The other main lobe corresponds to the angle at which the generatrix is perpendicular to the incident direction. Diffraction from the curved edges becomes important in the intermediate region between the main lobes. Finally, the simulated RCS results are compared with those from the measurement and good agreement can be seen.

## 2. Simulation of aircraft with inlets

In this section, the RCS of an aircraft's head with two engine inlets has been computed using HOB-MoM with the Out-of-Core algorithm. The models are shown in Fig.5. The canopy and radome are built as metal surface. The dimensions of the whole aircraft model are  $20\text{m} \times 15\text{m} \times 4.2\text{m}$ , and those of the aircraft's head with inlets are  $9.5\text{m} \times 4.6\text{m} \times 1.8\text{m}$ . Monostatic RCS in horizontal plane is computed at 1.6 GHz. Accordingly, the electrical sizes of the head model are  $51 \lambda \times 24.5 \lambda \times 9.6 \lambda$ .

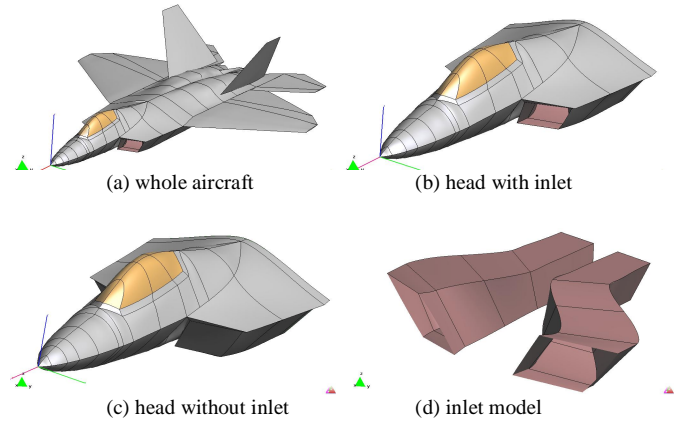


Figure 5. Aircraft and inlet model

Two different configurations of the aircraft's head are compared: the first is the model with inlets, and another is the model without inlets (the inlet mouth is closed by two metal plates). For the computational configuration, monostatic RCS on three planes of theta-cut ( $-10^\circ, 0^\circ, 10^\circ$ ) are computed, there are 121 phi angles ( $\phi = -60^\circ \sim 60^\circ$ ) for each theta-cut plane and the direction of  $\phi = 0^\circ$  is along the nose of the aircraft. In addition, mesh results and simulation setting are presented in Fig.6. Finally, the simulation results are shown in Fig.7. The blue line in which represents the results for the model with inlets, while the red one for the model without inlets.

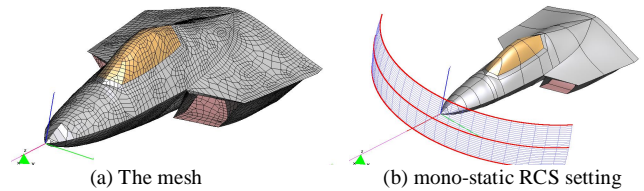
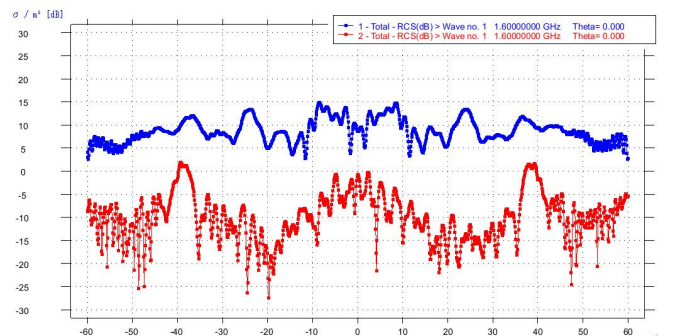


Figure 6. Mesh and computation setting

The number of unknowns by using HOB-MoM is 135315 and RAM required is about 273 GB. On the contrary, the number of unknowns produced by RWG MoM may reach the level of 2.7 million. The problem is simulated on a Lenovo workstation with 12 i7 CPU cores, totally 64 GB RAM and 4TB hard disk. 273GB hard disk is used to store the matrix; the RAM is used as the 'buffer' and it takes about 20 hours for simulating all the 363 angles.



## REFERENCES

- [1] R. F. Harrington, *Field Computation by Moment Methods*, IEEE Series on Electromagnetic Waves. New York: IEEE, 1993.
- [2] Y. Zhang and T.K. Sarkar, *Parallel solution of Integral Equation Based EM Problems in the Frequency Domain*. Hoboken, NJ: Wiley, 2009.
- [3] S.M. Rao, D.R. Wilton, and A.W. Glisson, "Electromagnetic scattering by surfaces of arbitrary shape", *IEEE Trans. Antennas Propagation*, vol. P-30, no.3: 409-418, 1982.
- [4] Zhang, Y., M. Taylor, T. K. Sarkar, H. Moon, and M.-T. Yuan, "Solving large complex problems using a higher-order basis: Parallel in-core and out-of-core integral-equation solvers", *IEEE Antennas and Propagation Mag.*, vol. 50, No. 4: 13-30, 2008.
- [5] Y. Zhang, M. Taylor, T. K. Sarkar, A. De, M.-T. Yuan, H. Moon, and C.-H. Liang, "Parallel in-core and out-of-core solution of electrically large problems using the RWG basis functions," *IEEE Antennas and Propagation Mag.*, vol. 50, no. 5: 84-94, 2008.
- [6] Y. Zhang, T. K. Sarkar, M. Taylor, and H. Moon, "Solving MoM problems with million level unknowns using a parallel out-of-core solver on a high performance cluster," *IEEE Antennas and Propagation Soc. Int. Symp.*, Charleston, SC, USA, 2009.
- [7] Ramesh Garg, *Analytical and Computational Methods in Electromagnetics*, Artech House, 2008.

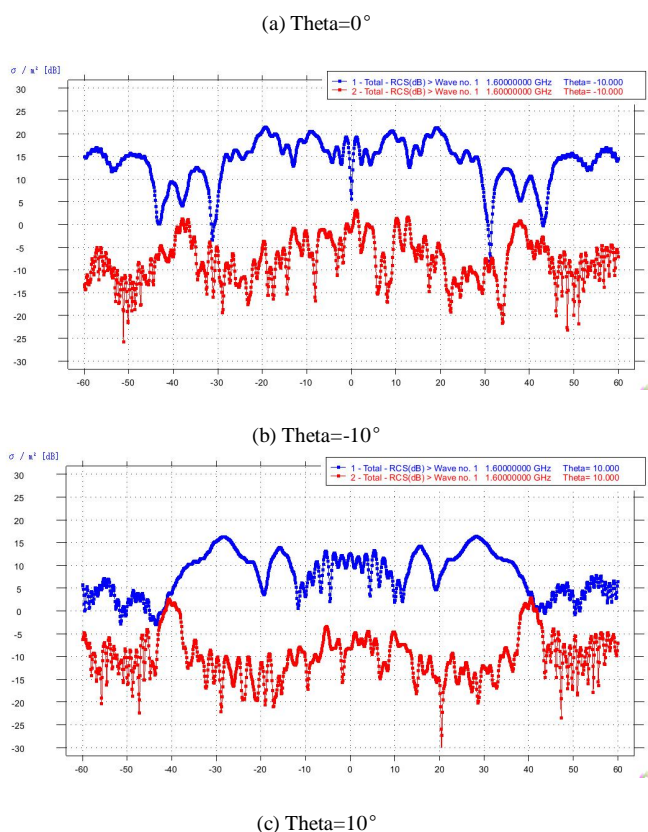


Figure 7. H polarization incidence mono-RCS (E-total)

Comparing those two results in upper pictures, we can find that the aircraft with inlets will produce larger monostatic RCS than that from the model without inlets. For different incident angles, the S-shaped inlets have the different scattering effect, which indicates that the inlet structures should be included for accurate simulation of the stealth aircraft.

## IV. CONCLUSION

In this paper, RCS computation of electrically large complex structures by using HOB-MoM with Out-of-Core technique is presented, which can successfully reduce the RAM required to store the MoM impedance matrix. Through the analysis of some numerical examples, the conclusion can be drawn that combining HOB-MoM and Out-of-Core technique can efficiently solve the electrically large problems which have strong resonance phenomenon, and this can not be achieved by the conventional RWG MoM.

## ACKNOWLEDGMENT

This work is partly supported by the National High Technology Research and Development Program ("863"Program) of China (2012AA01A308) and the NSFC (61072019).